Hybrid Aerogels

International Edition: DOI: 10.1002/anie.201507328
German Edition: DOI: 10.1002/ange.201507328

Strong, Thermally Superinsulating Biopolymer–Silica Aerogel Hybrids by Cogelation of Silicic Acid with Pectin

Shanyu Zhao, Wim J. Malfait, Arnaud Demilecamps, Yucheng Zhang, Samuel Brunner, Lukas Huber, Philippe Tingaut, Arnaud Rigacci, Tatiana Budtova, and Matthias M. Koebel**

Abstract: *Silica aerogels are excellent thermal insulators, but their brittle nature has prevented widespread application. To overcome these mechanical limitations, silica–biopolymer hybrids are a promising alternative. A one-pot process to monolithic, superinsulating pectin–silica hybrid aerogels is presented. Their structural and physical properties can be tuned by adjusting the gelation pH and pectin concentration. Hybrid aerogels made at pH 1.5 exhibit minimal dust release and vastly improved mechanical properties while remaining excellent thermal insulators. The change in the mechanical properties is directly linked to the observed "neck-free" nanoscale network structure with thicker struts. Such a design is superior to "neck-limited", classical inorganic aerogels. This new class of materials opens up new perspectives for novel silica–biopolymer nanocomposite aerogels.*

Silica aerogels are attractive candidates for thermal, catalytic, pharmaceutical, and chemical applications[1] because of their exceptional physical properties, such as low density ($0.1\,g\,cm^{-3}$) and thermal conductivity ($12–15\,mW\,m^{-1}\,K^{-1}$) and high porosity (>95%) and specific surface areas ($800–1000\,m^2\,g^{-1}$).[2] However, the widespread use of silica aerogels has been prevented by their poor mechanical properties[3] and concerns about dust release.[4] Silica aerogels are inherently fragile because of the weak pearl-necklace-like structure: the three-dimensional network consists of silica nanoparticles with diameters of 3–10 nm connected by narrow inter-particle necks.[5]

The preparation of silica aerogels with improved mechanical properties is well-documented. Three common routes to strengthen the gel network are: 1) chemical crosslinking with reactive molecules or polymers,[6] 2) impregnating or dispersing individual micro/nanoscopic secondary phases, such as polymers,[7] nanoparticles,[8] nanotubes,[9] or fibers,[10] into the silica matrix, and 3) using macroscopic fibrous templates made from polyester,[11] non-woven polypropylene,[12] fiberglass,[13] polyamide,[14] or electrospun polyurethane.[9] Among these strategies, chemical crosslinking with synthetic polymers (route 1) achieves the most significant improvement in the mechanical properties (ca. 40–900 MPa compressive modulus, 8–500 MPa compressive strength), but this reinforcement comes at the cost of a higher density ($0.3–0.8\,g\,cm^{-3}$), a decrease in porosity and surface area ($150–300\,m^2\,g^{-1}$), as well as a substantial increase in the thermal conductivity ($40–130\,mW\,m^{-1}\,K^{-1}$).[6a,c,15] Macroscopically reinforced polyethylene terephthalate and fiberglass (e.g., commercial Pyrogel) silica aerogel blankets (route 3) with thermal conductivities as low as $14\,mW\,m^{-1}\,K^{-1}$ are the most widely used aerogel-based products on the market today with an estimated market volume of $137.5 million per year.[16] However, some of today's commercial aerogel products can be dusty and offer only limited mechanical strength.

The use of bio-derived materials from renewable resources, such as proteins, polysaccharides, or plant oils,[17] decreases the overall carbon footprint of the products and reduces their environmental impact. Thus far, few reports have been published on the thermal conductivity of such bio-aerogels. Aeropectins are obtained by pectin dissolution, coagulation, and supercritical CO_2 drying. They display thermal conductivities between 16 and $22\,mW\,m^{-1}\,K^{-1}$ under ambient conditions.[18] Surface-carboxylated nanofibrillated cellulose aerogels display thermal conductivities as low as $18\,mW\,m^{-1}\,K^{-1}$.[1c] Several attempts were made to combine polysaccharide and silica phases with the goal of engineering nanostructured, strong, and thermally superinsulating aerogels. Cellulose–silica composite aerogels prepared by impregnation of a wet coagulated cellulose matrix with tetraethyl orthosilicate display increased specific surface areas[19] and Young's moduli,[19b] but also thermal conductivities above $25\,mW\,m^{-1}\,K^{-1}$. More recently, nanofibrillated cellulose was dispersed in or impregnated with silica-based sol and hydrophobized, and the resulting materials displayed excellent thermal properties, but only a moderate mechanical reinforcement.[20] Furthermore, a surface modification of the

[*] Dr. S. Zhao, Dr. W. J. Malfait, Dr. S. Brunner, L. Huber, Dr. M. M. Koebel
Building Energy Materials & Components Lab, EMPA
Swiss Federal Laboratories for Materials Science and Technology
CH-8600 Dübendorf (Switzerland)
E-mail: matthias.koebel@empa.ch
Dr. Y. Zhang
Electron Microscopy Center, EMPA
Swiss Federal Laboratories for Materials Science and Technology
CH-8600 Dübendorf (Switzerland)
Dr. P. Tingaut
Wood Laboratory, EMPA
Swiss Federal Laboratories for Materials Science and Technology
CH-8600 Dübendorf (Switzerland)
Dr. A. Demilecamps, Dr. T. Budtova
MINES ParisTech, PSL Research University
CEMEF - Centre de Mise en Forme des Matériaux
UMR CNRS 7635, CS 10207, 06904 Sophia Antipolis (France)
E-mail: tatiana.budtova@mines-paristech.fr
Dr. A. Rigacci
MINES ParisTech, PERSEE - Centre Procédés, Energies Renouvelables et Systèmes Energétiques, CS 10207
rue Claude Daunesse, 06904 Sophia Antipolis Cedex (France)

Supporting information for this article is available on the WWW under http://dx.doi.org/10.1002/anie.201507328.

cellulose nanofibers was necessary to improve the compatibility at the cellulose–silica interface.[20b]

Herein, we prepare nanoscale interpenetrating pectin–silica hybrid aerogels by dissolving pectin with a high methoxy (HM) content directly into an aqueous, water-glass-derived silicic acid solution, cogelation, solvent exchange, hydrophobization, and drying with supercritical CO_2 (Supporting Information, Figure S1). We systematically varied the pectin concentration and solution pH value, and designed a new class of pectin–silica hybrid aerogels with low thermal conductivity, tailored mechanical properties, and minimal dust release.

The success of this approach depends on controlling and matching the gelation kinetics of both phases (silica and polysaccharide), which depend on the pH value (Figure S2). Ion-exchanged sodium silicate solutions (silicic acid) are stable at $pH < 3$ (the gelation time at pH 1.5 is ca. 14 days), but gel within minutes at $pH > 4$. The gelation of HM pectin solutions with an esterification degree of 72 to 74% is very slow below pH 2.0 and takes 3–7 min[21] at $2 \le pH \le 3$, whereas no gelation occurs above pH 3.5. In this study, we prepared hybrid pectin–silica gels at pH 1.5 with very slow gelation of both components, at pH 3.0 with gelation of HM pectin within 10 min followed by slower gelation of the silicic acid phase,[21] and at pH 5.0 with no gelation of pectin but rapid gelation of the silica sol within 10 min.[22] The pectin/silica mass fractions were 5:100, 10:100, and 20:100, and the initial silica concentration was 7 wt%. After mixing, gelation, and aging, all samples were washed with ethanol, hydrophobized with hexamethyldisilazane (HMDS), and finally dried with supercritical CO_2 (see the Supporting Information for details on the overall procedure). The nomenclature of the samples is as follows: RS-X denotes the reference silica aerogels gelled at pH X, PecS-Y-X stands for the pectin–silica hybrids with pectin/silica weight ratios of Y:100 and gelled at pH X. The pectin loadings in the hybrids were confirmed by semi-quantitative Fourier transform infrared spectroscopy (Figure S3) and thermogravimetric analysis (Figure S4). Selected physical properties of all aerogels are listed in Table S1. In comparison with the reference silica aerogel, the presence of pectin increases the aerogel bulk density, slightly decreases the porosity, and increases the specific surface area, except for the formulations prepared at pH 5 (Figures S5, S6 and Table S1). For the same pectin loadings, the hybrids prepared at pH 1.5 have slightly higher ρ_{bulk} and S_{BET} values than the pH 3 and pH 5 samples (Table S1).

Scanning electron microscopy (SEM) revealed a 3D open porous network consisting of particle aggregates of tens of nanometers in size; fibrous structures could also be detected for some formulations (Figure 1). Neat silica aerogels are composed of aggregates of colloidal silica particles linked together in a pearl-necklace-type network structure.[23] Pure pectin aerogels display a network of polymer "strands" or "nanofibers" with diameters of a few tens of nanometers primarily with mesopores and small macropores.[19] The hybrids gelled at pH 1.5 do not show evidence of visible pectin "fibers" at all studied pectin concentrations (Figure 1 a, d, g). At this pH, pectin most probably did not completely gel within the preparation time. Hybrid aerogels prepared at pH 3 and pH 5 show a coarser microstructure than aerogels prepared at pH 1.5 for a given pectin loading. Aerogels with pectin concentrations above 10 wt% at pH 3

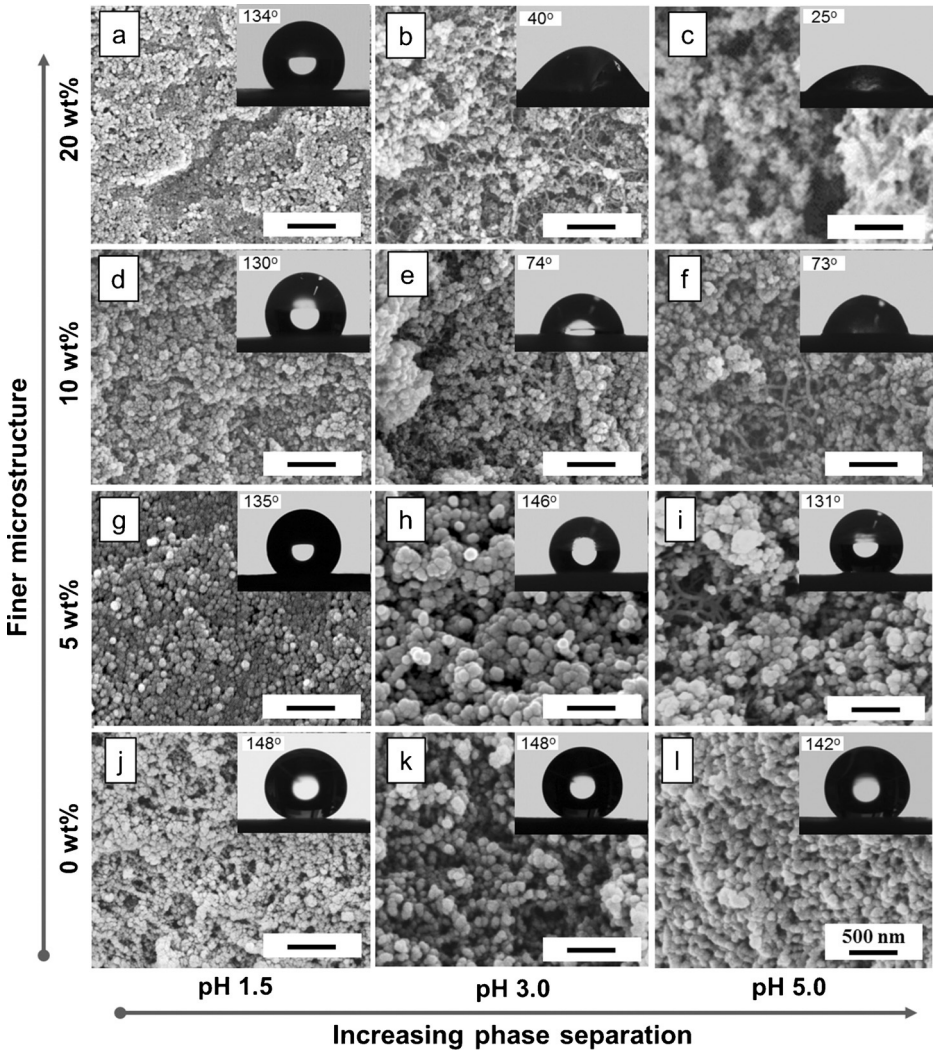

Figure 1. SEM images of the reference silica (0 wt% pectin) and pectin–silica hybrid aerogels prepared at various pH values and pectin concentrations. Scale bar: 500 nm, inset numbers are the water contact angles.

and 5 contain pectin nanofibers. At the highest pectin concentrations and pH values, the material segregates into biopolymer-rich and silica-rich domains (compare Figure 1b and c). For all investigated acidities, increasing the pectin content leads to finer microstructures with smaller silica secondary particles and pores, in agreement with the pore size analysis (Table S1, Figure S6).

The differences in the microstructure of the neat silica versus hybrid aerogels were clarified by high-resolution transmission electron microscopy (HRTEM). The pure silica aerogel displays a typical pearl-necklace structure with distinct quasi-spherical silica nanoparticles of 2–5 nm in diameter (Figure 2a). The cogelation with pectin at pH 1.5 leads to a drastic morphological change of the network structure (Figure 2b) towards a structure free of necks and with thicker and continuous struts. The formation of a polymer–silica hybrid with such a microstructure leads to a mechanically strong hybrid aerogel (see below). The hybrid gelled at high pH displays an inhomogeneous microstructure (Figures 2c and S8), consistent with the phase separation observed by SEM (Figure 1c). The PecS-20-1.5 hybrid aerogel features pore sizes on the order of a few tens of nanometers with pore wall thicknesses around 10 nm.

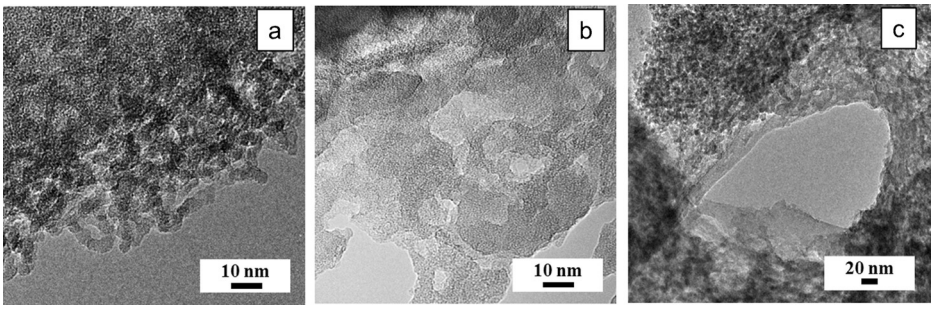

Figure 2. HRTEM images of a) the reference silica aerogel, b) PecS-20-1.5, and c) PecS-20-5.0.

We employed ^{1}H–^{29}Si heteronuclear correlation (HETCOR) solid-state NMR spectroscopy to confirm the homogenous distribution of silica and pectin in the PecS-20-1.5 sample (Figure 3). The spectrum displays the peaks typical for a silylated silica aerogel.[24] Furthermore, there is a correlation between the pectin protons (at 5–7 ppm) and Q^3 (Q^n is a tetrahedral Si atom with n bridging O atoms). The relative intensity of the pectin proton resonances is higher in the ^{1}H projection of the ^{1}H–^{29}Si HETCOR spectrum than in the quantitative ^{1}H spectrum. This increase in intensity is similar to the ethoxy (CH_2) protons where covalent $\equiv Si{-}O{-}CH_2{-}$ linkages exist. Compared to the spectrum of the pH 1.5 hybrid (Figure 3), these pectin Q^3 cross-peaks are less intense and absent in the spectra of the pH 5 hybrid and a macroscopic pectin–silica mixture, respectively (Figure S7). Thus, although the ^{1}H–^{29}Si HETCOR spectrum cannot, by definition, provide direct evidence for covalent silica–pectin bonds, it does provide unambiguous evidence that pectin and silica are interspersed on the molecular scale for samples gelled at low pH. The fine dispersion of pectin and silica is also evident from the TEM element maps (Figure S9).

To summarize the structural data, the morphology of pectin–silica hybrid aerogels is controlled by both pH value and pectin content. Slow gelation of both silica and pectin at pH 1.5 results in a homogenous spatial distribution of both components and a finer microstructure. At pH 3, pectin gels quickly[25] and forms a 3D network. This network can be seen in the SEM images of hybrids containing ≥ 10 wt% of pectin (Figure 1b,e). At pH 5, silica gels quickly, and pectin does not gel at all. The quick gelation of at least one of the components at pH > 2 results in heterogeneous hybrids with biopolymer-rich and silica-rich domains with larger pores (Figure 1c and Table S1) and, as will be shown later, less favorable mechanical properties when compared to hybrids prepared at pH 1.5. The presence of pectin reduces the size of the silica secondary particles and pores, most likely owing to the stabilizing complexation interaction of the biopolymer with the hydrophilic silica surface.

The pronounced alteration of the microstructure with pectin addition dramatically changes the physical and mechanical properties (Figures S9–S11). Unlike reference silica aerogels, hybrid aerogels prepared at pH 1.5 can sustain uniaxial compression to at least 80% strain without rupture (Figure S10). The compressive elastic modulus (E), the final strength (σ_{max}), and the fracture strain (ε_f) strongly depend on the pectin loading and the gelation pH, with the most significant improvement observed for the hybrids prepared at pH 1.5 (Figures 4a,b and S11). The mechanical reinforcement at pH 1.5 is also evident from the BET isotherms (Figure S5a): the hybrid materials present almost no mechanical-deformation-induced hysteresis, which indicates that the hybrids maintain their morphological integrity during liquid nitrogen desorption.[3]

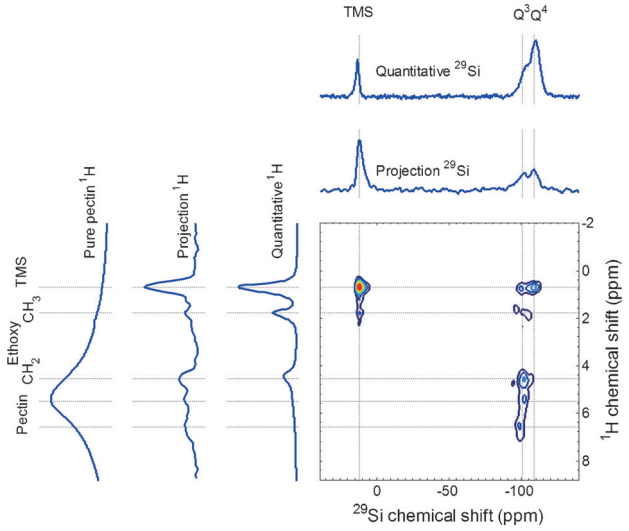

Figure 3. ^{1}H–^{29}Si heteronuclear correlation NMR spectrum for PecS-20-1.5.

Another major advantage of the pectin–silica hybrids is their limited dust release, which is lower than that of the

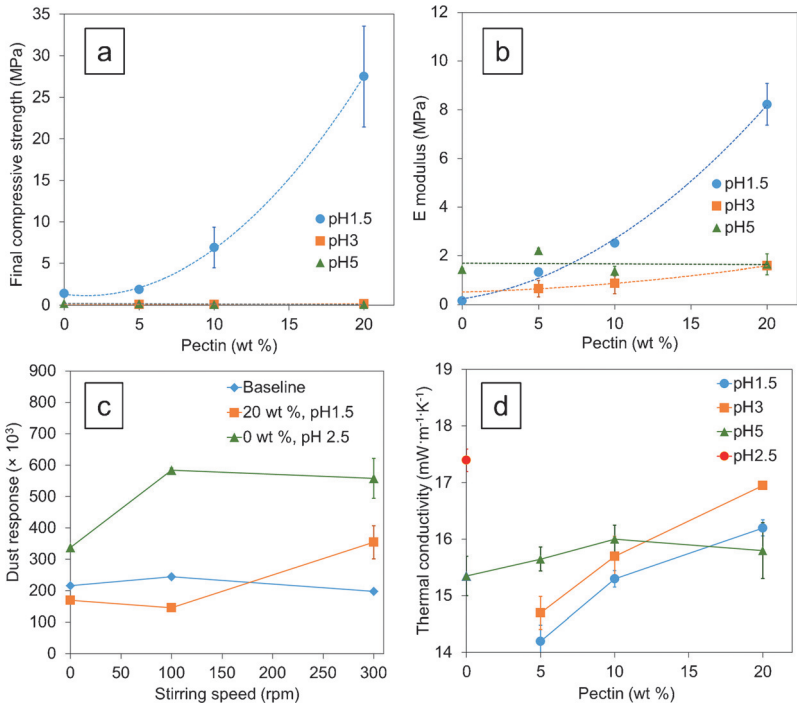

Figure 4. a) Final compressive strength (σ_{max}). b) Compressive modulus (E). c) Submicrometer (< 500 nm) particle dust release during mechanical grinding of RS-2.5 and PecS-20-1.5. d) Thermal conductivity. The pH 2.5 silica aerogel was used as a reference because the pH 1.5 silica aerogel was extremely fragile.

reference silica aerogel by a factor of two to ten (Figures 4c and S13). The mechanical reinforcement and minimal dust release correlate well with the microstructural observations, with the best properties observed for the pectin-rich, homogeneous, neck-free hybrids synthesized at pH 1.5 (Figures 2 and 3). Aside from this morphological change, well-dispersed pectin molecules may strengthen the material through hydrogen bonding to silanol groups. Hybridization at higher pH does not improve the mechanical properties because of pectin aggregation and the formation of fibrous network structures (Figure 1).

One of the main applications of aerogels is in high-performance thermal insulation. The thermal conductivity (λ) was measured on monolithic $48 \times 48 \times (6–8)$ mm^3 tiles at 25 °C and 50 % relative humidity (RH).[26] At pH 1.5, the sample with a minimal pectin loading of 5 wt % showed the lowest conductivity of the whole series, 14.2 mW m^{-1} K^{-1}. Increasing the pectin content increases the thermal conductivity owing to the higher solid conductivity and water uptake (Figure 4d), but this increase is very minor, and all hybrid aerogels are superinsulating with λ values between 14 and 17 mW m^{-1} K^{-1}.[27] This outstanding thermal performance places this new class of hybrids amongst the best thermal insulators under ambient conditions, but with drastically improved mechanical properties. Pectin–silica hybrids prepared at pH 1.5 thus present a unique combination of very low thermal conductivity and superior final compressive strength. Importantly, the pectin–silica hybrids offer a far superior insulation performance compared to state-of-the-art silica hybrid aerogels reinforced by isocyanate, epoxy, chitosan, and cellulose at comparable densities (Figure 5)[3, 6a, 18–19, 20b, 28].

Apart from the mechanical strength and thermal conductivity, durability is another key feature for aerogel applications. Thermogravimetric analysis (Figure S4) demonstrates that the pectin–silica hybrids are stable up to 250 °C, and that the pectin and trimethylsilyl groups decompose around 270 and 600 °C, respectively. Hydrophobicity is another key parameter. The reference silylated silica aerogels show high contact angles ($\theta > 140°$) regardless of pH, but the contact angle is pH-dependent for the pectin–silica hybrids: high contact angles ($\theta > 130°$) are maintained at pH 1.5 (Table S1, Figure 1), but a significant loss of surface hydrophobicity ($\theta < 90°$) occurs for hybrid aerogels prepared at pH 3 and pH 5 at higher pectin concentrations, most probably because of the presence of pectin-rich domains. In contrast, the humidity uptake is independent of pH, but strongly depends on pectin content (Figure S14a). The pectin–silica hybrids display a moderate humidity uptake of 5–6 % at 80 % RH compared to non-hydrophobized silica and pure pectin aerogels, with about 20–30 % moisture uptake (Figure S14b). The contrasting pH dependence of the contact angle and humidity uptake indicates that the hydrophobicity is linked both to the pH-dependent microstructure (Figure 1) and to the inherent chemical hydrophobicity.

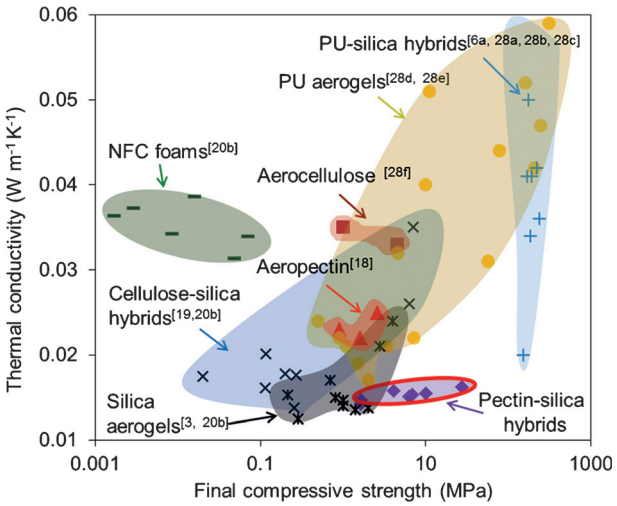

Figure 5. Thermal conductivity versus final compressive strength for aerogel-like materials. The compressive strengths of NFC foams, aeropectin, and part of PU aerogels and aerocellulose were taken at 50 % strain.

In conclusion, the homogenous, mesoporous, neck-free structure of pectin–silica hybrids prepared in a one-pot process at pH 1.5 leads to high compressive strength, high stiffness, and minimal dust release without compromising the thermal superinsulating properties. The resulting materials

not only surpass current state-of-the-art composites with their unique hydrophobic, thermal, and mechanical properties, but are also derived from bio-based precursors through an attractive aqueous "green" process. As a broad library of polysaccharides are commercially available, this study not only opens up new prospects for developing high-performance, commercially scalable hybrid aerogels for engineering and biological applications, but also offers insight into structure–property aspects of three-dimensional nanoscale interpenetrating hybrid aerogel materials.

Acknowledgements

This work was financially supported by the European Commission under the Seventh Framework Program (Call identifier: EeB.NMP.2010-1, Contract No. 260141, Aerocoins project: http://www.aerocoins.eu). We thank Beatrice Fischer for her assistance with the mechanical testing and FTIR and TGA measurements, Rene Verel for his assistance with the NMR measurements, and Eunho Jeong and Stefanie Hauser for their help with the sample preparation. The authors declare no competing financial interest.

Keywords: hybrid aerogels · NMR spectroscopy · polysaccharides · transmission electron microscopy

How to cite: *Angew. Chem. Int. Ed.* **2015**, *54*, 14282–14286
Angew. Chem. **2015**, *127*, 14490–14494

[1] a) A. C. Pierre, G. M. Pajonk, *Chem. Rev.* **2002**, *102*, 4243–4266; b) I. Smirnova in *Aerogel handbook* (Eds.: M. A. Aegerter, N. Leventis, M. M. Koebel), Springer, New York, **2011**, pp. 695–717; c) Y. Kobayashi, T. Saito, A. Isogai, *Angew. Chem. Int. Ed.* **2014**, *53*, 10394–10397; *Angew. Chem.* **2014**, *126*, 10562–10565.

[2] a) M. A. Aegerter, N. Leventis, M. M. Koebel, *Aerogels handbook*, Springer, New York, **2011**; b) S. S. Prakash, J. C. Brinker, A. J. Hurd, S. M. Rao, *Nature* **1995**, *375*, 431–431; c) S. S. Kistler, *Nature* **1931**, *127*, 741–741.

[3] J. C. H. Wong, H. Kaymak, S. Brunner, M. M. Koebel, *Microporous Mesoporous Mater.* **2014**, *183*, 23–29.

[4] a) S. Ratynskaia, H. Bergsåker, B. Emmoth, A. Litnovsky, A. Kreter, V. Philipps, *Nucl. Fusion* **2009**, *49*, 122001; b) H. F. Krug, *Angew. Chem. Int. Ed.* **2014**, *53*, 12304–12319; *Angew. Chem.* **2014**, *126*, 12502–12518.

[5] N. Hüsing, U. Schubert, *Angew. Chem. Int. Ed.* **1998**, *37*, 22–45; *Angew. Chem.* **1998**, *110*, 22–47.

[6] a) A. Katti, N. Shimpi, S. Roy, H. Lu, E. F. Fabrizio, A. Dass, L. A. Capadona, N. Leventis, *Chem. Mater.* **2006**, *18*, 285–296; b) W. Yin, S. Venkitachalam, E. Jarrett, S. Staggs, N. Leventis, H. Lu, D. Rubenstein, *J. Biomed. Mater. Res. Part A* **2010**, *92*, 1431–1439; c) B. N. Nguyen, M. A. B. Meador, A. Medoro, V. Arendt, J. Randall, L. McCorkle, B. Shonkwiler, *ACS Appl. Mater. Interfaces* **2010**, *2*, 1430–1443; d) N. Leventis, *Acc. Chem. Res.* **2007**, *40*, 874–884; e) H. Maleki, L. Duraes, A. Portugal, *J. Mater. Chem. A* **2015**, *3*, 1594–1600.

[7] A. Demilecamps, G. Reichenauer, A. Rigacci, T. Budtova, *Cellulose* **2014**, *21*, 2625–2636.

[8] a) Y. Duan, The University of Akron (Ann Arbor), **2012**; b) M. F. Bertino, J. F. Hund, G. Zhang, C. Sotiriou-Leventis, A. T. Tokuhiro, N. Leventis, *J. Sol-Gel Sci. Technol.* **2004**, *30*, 43–48.

[9] L. Li, B. Yalcin, B. N. Nguyen, M. A. B. Meador, M. Cakmak, *ACS Appl. Mater. Interfaces* **2009**, *1*, 2491–2501.

[10] a) A. K. Bledzki, J. Gassan, *Prog. Polym. Sci.* **1999**, *24*, 221–274; b) L. Franzel, C. Wingfield, M. F. Bertino, S. Mahadik-Khanolkar, N. Leventis, *J. Mater. Chem. A* **2013**, *1*, 6021–6029.

[11] J. K. Lee, US patent US20070259979A1, **2007**.

[12] Z. Zhang, J. Shen, X. Ni, G. Wu, B. Zhou, M. Yang, X. Gu, M. Qian, Y. Wu, *J. Macromol. Sci. Part A* **2006**, *43*, 1663–1670.

[13] B. Yuan, S. Ding, D. Wang, G. Wang, H. Li, *Mater. Lett.* **2012**, *75*, 204–206.

[14] D. H. Blount, US Patent US4954327A, **1990**.

[15] M. A. B. Meador in *Aerogels Handbook* (Eds.: M. A. Aegerter, N. Leventis, M. M. Koebel), Springer, New York, **2011**, pp. 315–334.

[16] BCC research Inc, Wellesley, MA, USA, **2013**.

[17] a) Y.-D. Li, J.-B. Zeng, X.-L. Wang, K.-K. Yang, Y.-Z. Wang, *Biomacromolecules* **2008**, *9*, 3157–3164; b) M. A. R. Meier, J. O. Metzger, U. S. Schubert, *Chem. Soc. Rev.* **2007**, *36*, 1788–1802; c) S.-D. Zhang, Y.-R. Zhang, X.-L. Wang, Y.-Z. Wang, *Starch/Staerke* **2009**, *61*, 646–655.

[18] C. Rudaz, R. Courson, L. Bonnet, S. Calas-Etienne, H. Sallée, T. Budtova, *Biomacromolecules* **2014**, *15*, 2188–2195.

[19] a) J. Cai, S. Liu, J. Feng, S. Kimura, M. Wada, S. Kuga, L. Zhang, *Angew. Chem. Int. Ed.* **2012**, *51*, 2076–2079; *Angew. Chem.* **2012**, *124*, 2118–2121; b) A. Demilecamps, C. Beauger, C. Hildenbrand, A. Rigacci, T. Budtova, *Carbohydr. Polym.* **2015**, *122*, 293–300.

[20] a) G. Hayase, K. Kanamori, K. Abe, H. Yano, A. Maeno, H. Kaji, K. Nakanishi, *ACS Appl. Mater. Interfaces* **2014**, *6*, 9466–9471; b) S. Zhao, Z. Zhang, G. Sèbe, R. Wu, R. V. Rivera Virtudazo, P. Tingaut, M. M. Koebel, *Adv. Funct. Mater.* **2015**, *25*, 2326–2334.

[21] J. F. Thibault, M. C. Ralet in *Advances in Pectin and Pectinase Research* (Eds.: F. Voragen, H. Schols, R. Visser), Springer, Dordrecht, Netherlands, **2004**, pp. 91–105.

[22] R. V. Rao, G. M. Pajonk, Uzma K. H. Bangi, A. Parvathy Rao, M. M. Koebel in *Aerogel handbook* (Eds.: M. A. Aegerter, N. Leventis, M. M. Koebel), Springer, New York, **2011**, pp. 118–119.

[23] H. Maleki, L. Duraes, A. Portugal, *J. Non-Cryst. Solids* **2014**, *385*, 55–74.

[24] W. J. Malfait, R. Verel, M. M. Koebel, *J. Phys. Chem. C* **2014**, *118*, 25545–25554.

[25] S. E. Harding, G. Berth, A. Ball, J. R. Mitchell, J. G. de La Torre, *Carbohydr. Polym.* **1991**, *16*, 1–15.

[26] T. Stahl, S. Brunner, M. Zimmermann, K. Ghazi Wakili, *Energ. Buildings* **2012**, *44*, 114–117.

[27] M. Koebel, A. Rigacci, P. Achard in *Aerogels Handbook* (Eds.: M. A. Aegerter, N. Leventis, M. M. Koebel), Springer, New York, **2011**, pp. 607–633.

[28] a) G. Churu, B. Zupančič, D. Mohite, C. Wisner, H. Luo, I. Emri, C. Sotiriou-Leventis, N. Leventis, H. Lu, *J. Sol-Gel Sci. Technol.* **2015**, *75*, 98–123; b) K.-J. Chang, Y.-Z. Wang, K.-C. Peng, H.-S. Tsai, J.-R. Chen, C.-T. Huang, K.-S. Ho, W.-F. Lien, *J. Polym. Res.* **2014**, *21*, 1–9; c) M. A. B. Meador, L. A. Capadona, L. McCorkle, D. S. Papadopoulos, N. Leventis, *Chem. Mater.* **2007**, *19*, 2247–2260; d) C. Chidambareswarapattar, P. M. McCarver, H. Luo, H. Lu, C. Sotiriou-Leventis, N. Leventis, *Chem. Mater.* **2013**, *25*, 3205–3224; e) N. Diascorn, S. Calas, H. Sallée, P. Achard, A. Rigacci, *J. Supercrit. Fluids,* DOI: 10.1016/j.supflu.2015.05.012; f) R. Sescousse, R. Gavillon, T. Budtova, *Carbohydr. Polym.* **2011**, *83*, 1766–1774.

Received: August 6, 2015
Published online: October 8, 2015

